Dynamics of nuclear spin measurement in a mesoscopic solid-state quantum computer

2000 J. Phys.: Condens. Matter 12 2945

(http://iopscience.iop.org/0953-8984/12/13/306)

J. Phys.: Condens. Matter **12** (2000) 2945–2952. Printed in the UK PII: S0953-8984(00)09052-4

Dynamics of nuclear spin measurement in a mesoscopic solid-state quantum computer

Gennady P Berman†, David K Campbell†‡, Gary D Doolen† and Kirill E Nagaev†§

† Theoretical Division and CNLS, Los Alamos National Laboratory, Los Alamos, NM 87545, USA

‡ Department of Physics, University of Illinois at Urbana-Champaign, 1110 West Green Street, Urbana, IL 61801-3080, USA

§ Institute of Radioengineering and Electronics, Russian Academy of Sciences, Mokhovaya Street 11, 103907 Moscow, Russia

Received 28 October 1999

Abstract. We study numerically the process of nuclear spin measurement in a solid-state quantum computer of the type proposed by Kane, by calculating the quantum dynamics of two coupled nuclear spins on ^{31}P donors implanted in ^{28}Si. We estimate the time of the 'quantum swap operation'—the minimum measurement time required for the reliable transfer of quantum information from the nuclear spin subsystem to the electronic subsystem. Our calculations show that for realistic values of the parameters this time is of the order of $\tau_{swap} \sim 5 \times 10^{-5}$ s. We also calculate the probability of error for typical values of the external noise.

1. Introduction

Recently, a new implementation of a solid-state quantum computer was proposed by Kane [1]. Kane's idea is to use nuclear spins of ^{31}P donors in silicon as the quantum bits (qubits). These 1/2 spins are known to exhibit very large relaxation times because of their poor contact with the environment [2]. At low temperatures, when there are no thermally excited electrons in the conduction band, this interaction with the environment is mediated primarily by the magnetic field and hyperfine interaction with s electrons localized on the donor. However, not all s electrons are equally important for this mediation. The electrons of inner shells are localized within one lattice cell and are also relatively weakly coupled with the environment. Of five outer electrons owned by a ^{31}P atom (one more than ^{28}Si), four form valence bonds with surrounding ^{28}Si atoms, while the fifth is given to the conduction band to form a loosely bound hydrogen-like s state in the field of the positively charged donor. Since the motion of this electron is described in terms of the effective mass, which is small in semiconductors, its localization radius is as large as 30 Å. Hence its state may be controlled by relatively moderate electric fields. On the other hand, the exchange interaction between loosely bound electrons located on different donors results in a weak indirect coupling between their nuclear spins [3], which is necessary for performing, e.g., the quantum 'control–not' operation.

A schematic illustration of the quantum computer proposed by Kane is shown in figure 1, for a two-qubit realization. Two ^{31}P donors are implanted in silicon and subjected to an external dc magnetic field of about $B = 2$ T. This creates a Zeeman splitting of the nuclear spin levels of about 3.5×10^7 Hz, and the Zeeman splitting of electron levels of about 5.6×10^{10} Hz (much

0953-8984/00/132945+08$30.00

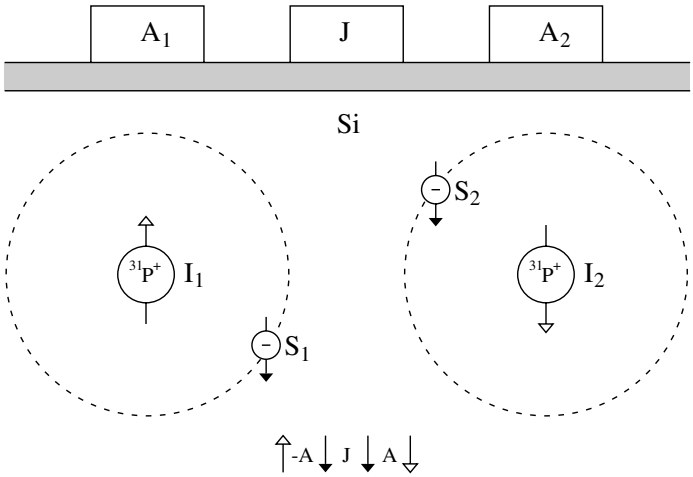

Figure 1. Two ^{31}P donors in silicon. The nuclear spins are coupled to the outer electrons by the hyperfine interactions, which can be controlled by the A-gates. The electrons are mutually coupled via the exchange interaction, which can be controlled by the J-gate.

smaller than the splitting between the ground and the lowest excited hydrogen-like states of an electron, which is 15 meV [4, 5]). The hyperfine coupling constant for ^{28}Si:^{31}P is 29 MHz. Since this constant is proportional to the probability of finding the electron near the nuclei, it can be decreased by effects that attract the electron away from the ^{31}P nucleus, which in the device depicted in figure 1 can be accomplishment by applying a positive voltage to the gates labelled A_1 and A_2. Similarly, the exchange interaction between the electrons located on different donors may be controlled by applying positive or negative voltage to the J-gate in figure 1, thereby changing the overlap of the electron wave functions.

In this article, we do not consider the actual *process* of quantum computation, but instead focus on the *retrieving* of the result after the computation has been completed. The weak coupling of the nuclear spins with their environment, which is essential to avoid the decoherence that will spoil the quantum computation, makes this retrieval a highly nontrivial task. In particular, it cannot be achieved by means of existing NMR methods, since their sensitivity is insufficient for detecting the signal from a single nuclear spin. Recognizing this, Kane proposed in reference [1] a special measurement procedure based on transferring the information about the spin state of the system to its *charge* state—a 'quantum swap operation'. (See also reference [6] which addresses the measurement of an isolated nuclear spin on a single Te atom instead of the relative state of two coupled nuclear spins.) In the following, we simulate the measurement procedure proposed by Kane in reference [1] and estimate its optimal duration and minimum probability of error. In spite of the fact that the process of measurement is supposed to be adiabatic, we do not use in our analysis the adiabatic approximation. Since the system exhibits a level-crossing behaviour, this approximation is inapplicable, and we have to solve the equations numerically.

2. Eigenenergies and eigenstates

The Hamiltonian of the system is

$$\mathcal{H} = 2\mu_B B(\hat{S}_{1z} + \hat{S}_{2z}) - 2g_n\mu_n B(\hat{I}_{1z} + \hat{I}_{2z}) + 4A_1\hat{\boldsymbol{S}}_1 \cdot \hat{\boldsymbol{I}}_1 + 4A_2\hat{\boldsymbol{S}}_2 \cdot \hat{\boldsymbol{I}}_2 + 4J\hat{\boldsymbol{S}}_1 \cdot \hat{\boldsymbol{S}}_2 \qquad (1)$$

where $\hat{\boldsymbol{S}}_i$ and $\hat{\boldsymbol{I}}_i$ are electron and nuclear spin operators corresponding to donors 1 and 2, μ_B and μ_n are the Bohr and nuclear magnetons, $g_n = 1.13$ is the nuclear g-factor, B is the external magnetic field, A_i are the hyperfine interaction constants for nuclei 1 and 2, and J is the constant of exchange interaction between the electrons.

The Hamiltonian $\mathcal{H}$ can be represented by a 16×16 matrix in the basis of states with definite electron and nuclear spin projections. Since the total projection of the spin on the field direction is conserved, all possible states fall into five invariant subspaces, corresponding to its values -2, -1, 0, 1, and 2. In what follows, we will be interested only in the states with $S_{z\Sigma} + I_{z\Sigma} = -1$, which are used for measuring the nuclear spin states. Hence we may focus on the following reduced basis of four states: $|{\downarrow\downarrow}\rangle_e|{\downarrow\uparrow}\rangle_n$, $|{\downarrow\downarrow}\rangle_e|{\uparrow\downarrow}\rangle_n$, $|{\downarrow\uparrow}\rangle_e|{\downarrow\downarrow}\rangle_n$, and $|{\uparrow\downarrow}\rangle_e|{\downarrow\downarrow}\rangle_n$. In the reduced basis, the Hamiltonian can be represented by the 4×4 matrix

$$\mathcal{H} = \begin{pmatrix} J - 2\mu_B B & 0 & 2A_1 & 0 \\ 0 & J - 2\mu_B B & 0 & 2A_2 \\ 2A_1 & 0 & 2g_n\mu_n B - J & 2J \\ 0 & 2A_2 & 2J & 2g_n\mu_n B - J \end{pmatrix}. \tag{2}$$

For simplicity, we henceforth assume that $A_1 = A_2 = A$. Then the Hamiltonian is symmetric with respect to donors 1 and 2 and the eigenstates are either symmetric or antisymmetric with respect to interchanging them. The two symmetric states, $|E_1\rangle$ and $|E_2\rangle$, have total electron and nuclear spins $\boldsymbol{S}_\Sigma = 1$ and $\boldsymbol{I}_\Sigma = 1$. The corresponding eigenenergies are given by

$$E_1 = g_n\mu_n B + J - \mu_B B + \sqrt{(\mu_B B + g_n\mu_n B)^2 + 4A^2} \tag{3}$$

$$E_2 = g_n\mu_n B + J - \mu_B B - \sqrt{(\mu_B B + g_n\mu_n B)^2 + 4A^2} \tag{4}$$

and the corresponding (unnormalized) eigenvectors are

$$|E_1\rangle = -(2g_n\mu_n B + J - E_1)|{\downarrow\downarrow}\rangle_e|{\downarrow\uparrow} + {\uparrow\downarrow}\rangle_n + 2A|{\downarrow\uparrow} + {\uparrow\downarrow}\rangle_e|{\downarrow\downarrow}\rangle_n \tag{5}$$

$$|E_2\rangle = -(2g_n\mu_n B + J - E_2)|{\downarrow\downarrow}\rangle_e|{\downarrow\uparrow} + {\uparrow\downarrow}\rangle_n + 2A|{\downarrow\uparrow} + {\uparrow\downarrow}\rangle_e|{\downarrow\downarrow}\rangle_n. \tag{6}$$

The eigenenergies E_1 and E_2 are linear functions of J (see figure 2) and the structure of the corresponding eigenstates is independent of J (see figure 3).

The Hamiltonian $\mathcal{H}$ also has two antisymmetric states, $|E_3\rangle$ and $|E_4\rangle$, with total spin $\boldsymbol{S}_\Sigma + \boldsymbol{I}_\Sigma = 1$. The energies E_3 and E_4 are given by

$$E_3 = g_n\mu_n B - J - \mu_B B + \sqrt{(\mu_B B + g_n\mu_n B - 2J)^2 + 4A^2} \tag{7}$$

$$E_4 = g_n\mu_n B - J - \mu_B B - \sqrt{(\mu_B B + g_n\mu_n B - 2J)^2 + 4A^2}. \tag{8}$$

The corresponding (unnormalized) eigenvectors are

$$|E_3\rangle = -2A|{\downarrow\downarrow}\rangle_e|{\downarrow\uparrow} - {\uparrow\downarrow}\rangle_n - (2\mu_B B - J + E_3)|{\downarrow\uparrow} - {\uparrow\downarrow}\rangle_e|{\downarrow\downarrow}\rangle_n \tag{9}$$

$$|E_4\rangle = -2A|{\downarrow\downarrow}\rangle_e|{\downarrow\uparrow} - {\uparrow\downarrow}\rangle_n - (2\mu_B B - J + E_4)|{\downarrow\uparrow} - {\uparrow\downarrow}\rangle_e|{\downarrow\downarrow}\rangle_n. \tag{10}$$

Unlike the energies of symmetric states, E_3 and E_4 are nonmonotonic functions of J (see figure 2). If A were zero, the $E_3(J)$ and $E_4(J)$ curves would intersect at $J = \mu_B B/2$. However, since these terms have the same symmetry, they repel to form an avoided crossing in the form of a 'bottleneck' of width $4A$ at the would-be intersection point (see figure 2, inset). The corresponding eigenvectors also undergo restructuring at this point. That is, as J increases from $J < \mu_B B/2$ to $J > \mu_B B/2$, $|E_3\rangle$ transforms from $|{\downarrow\uparrow} - {\uparrow\downarrow}\rangle_e|{\downarrow\downarrow}\rangle_n$ with $\boldsymbol{S}_\Sigma = 0$ and $\boldsymbol{I}_\Sigma = 1$ into $|{\downarrow\downarrow}\rangle_e|{\downarrow\uparrow} - {\uparrow\downarrow}\rangle_n$ with $\boldsymbol{S}_\Sigma = 1$ and $\boldsymbol{I}_\Sigma = 0$. In other words, the electron and neutron subsystems exchange their spins. Simultaneously, $|E_4\rangle$ undergoes the inverse transformation from $|{\downarrow\downarrow}\rangle_e|{\downarrow\uparrow} - {\uparrow\downarrow}\rangle_n$ into $|{\downarrow\uparrow} - {\uparrow\downarrow}\rangle_e|{\downarrow\downarrow}\rangle_n$ with the opposite spin transfer.

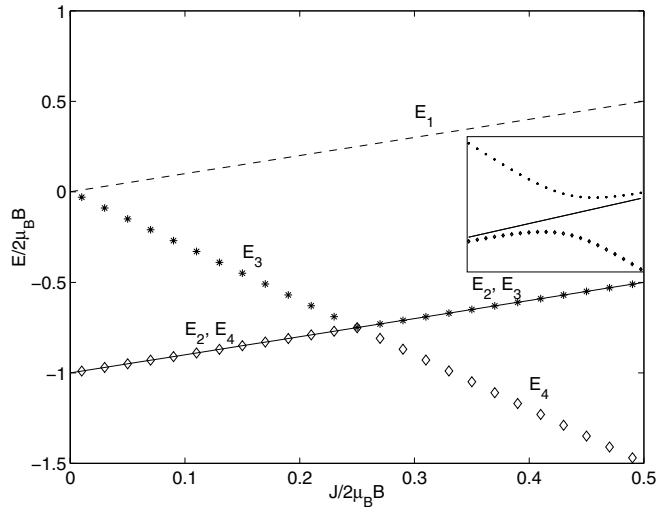

Figure 2. Energy levels of the system of two coupled nuclear and electron spins versus the exchange coupling J. The inset provides an expanded-scale view of the avoided crossing ('bottleneck') formed by the $E_3(J)$ and $E_4(J)$ curves at $J = \mu_B B/2$.

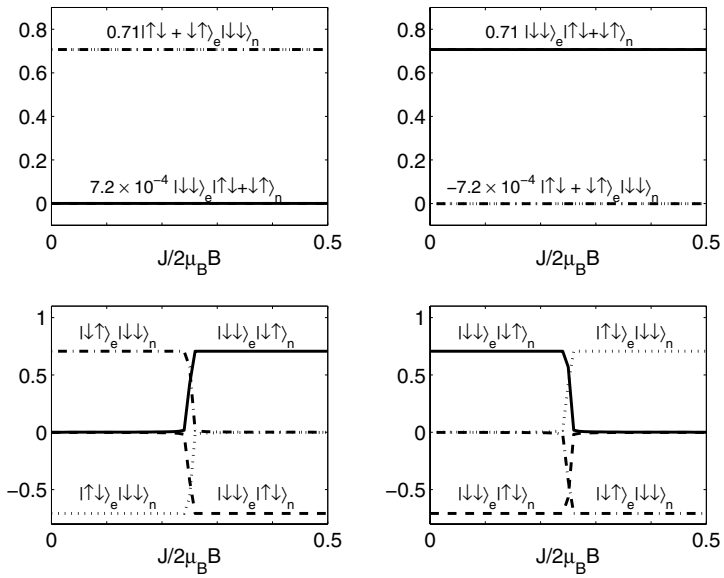

Figure 3. The components of the $|E_1\rangle$, $|E_2\rangle$, $|E_3\rangle$, and $|E_4\rangle$ states versus J.

One can thus distinguish between the singlet and triplet states of the nuclear subsystem as follows. Suppose that after the quantum computation has been performed at $J \to 0$, the electron subsystem is in the $|\downarrow\downarrow\rangle_e$ state. Then the whole system is either in the $|E_2\rangle$ or in the $|E_4\rangle$ state depending on whether the nuclear subsystem is in the $|\downarrow\uparrow + \uparrow\downarrow\rangle_n$ or the $|\downarrow\uparrow - \uparrow\downarrow\rangle_n$ state. If the exchange parameter, J, is then adiabatically increased to $J \gg \mu_B B/2$, the final electron subsystem becomes (respectively) a triplet or singlet state, thus allowing the information to be transferred from the nuclear to the electron spin subsystem. To accomplish

the measurement, one can distinguish between these electron spin states through the difference in their charge properties as described by Kane [1].

3. Simulations of the measurement dynamics

To simulate the dynamics of the measurement, we numerically solve the equation

$$\frac{\mathrm{d}\rho}{\mathrm{d}t} = \frac{\mathrm{i}}{\hbar}[\rho, \mathcal{H}(t) + \delta\mathcal{H}(t)] \tag{11}$$

where ρ is the 4×4 density matrix of the system and $\mathcal{H}(t)$ is given by (1) with $J(t)$ linearly increasing from 0 to $2\mu_B B$. We allow the fluctuating error

$$\delta\mathcal{H} = 4\,\delta A_1(t)\hat{\boldsymbol{S}}_1 \cdot \hat{\boldsymbol{I}}_1 + 4\,\delta A_2(t)\hat{\boldsymbol{S}}_2 \cdot \hat{\boldsymbol{I}}_2 \tag{12}$$

to account for voltage noise in the A-gates. The random classical quantities δA_1 and δA_2 are assumed to have zero averages and correlation time, τ_c, much shorter than all the dynamic timescales. Following Abragam [7], we may rewrite the equation for the density matrix in the form

$$\frac{\mathrm{d}\rho}{\mathrm{d}t} = -\frac{\mathrm{i}}{\hbar}[\mathcal{H}, \rho] - \frac{\tau_c}{\hbar^2}\overline{[\delta\mathcal{H}(t), [\delta\mathcal{H}(t), \rho]]} \tag{13}$$

where the horizontal bar denotes averaging over realizations of the fluctuations. We estimate the spectral density of fluctuations of A_1 and A_2 using the spectral density of voltage fluctuations for room-temperature electronics: $S_V = 10^{-18}\ \mathrm{V^2\,Hz^{-1}}$ and $\mathrm{d}A/\mathrm{d}V \sim 30\,\mathrm{MHz\,V^{-1}}$ (see [1]). The system is assumed to be initialized in the $|E_4\rangle$ state.

Figure 4 shows the time dependencies of the occupation probabilities of the eigenstates $|E_1\rangle$–$|E_4\rangle$ for the duration of the measurement during the measurement process. In the figure,

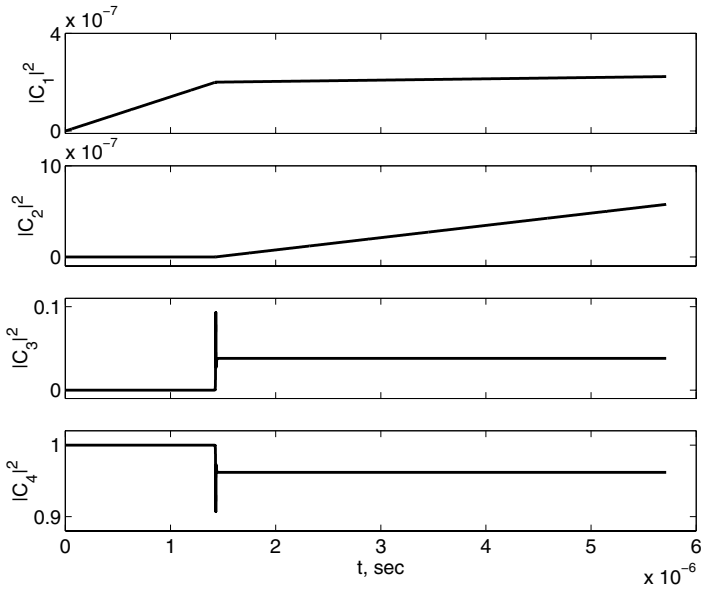

Figure 4. The time evolution of the occupancies of the $|E_1\rangle$–$|E_4\rangle$ states during the measurement ($0 \leqslant t \leqslant T$). The quantities $C_i(t)$ denote the expansion coefficients of the wave function in terms of the eigenstates $|E_i\rangle$. The duration of the measurement is $T = 5.7 \times 10^{-6}$ s, the hyperfine interaction constant is $A/h = 2.9 \times 10^7$ Hz, and the noise spectral density is $S_A/h^2 = 3.5 \times 10^{-3}$ Hz.

we have taken the duration of the measurement to be $T = 5.7\times10^{-6}$ s, the hyperfine interaction constant to be $A/h = 2.9\times10^{7}$ Hz, and the noise spectral density to be $S_A/h^2 = 3.5\times10^{-3}$ Hz. It is readily seen that increasing J at a finite rate results in a finite probability of exciting the system from $|E_4\rangle$ into $|E_3\rangle$, creating one source of measurement error. Another source of error is noise-induced 'escape' into $|E_1\rangle$ and $|E_2\rangle$ states. Note that the system cannot be excited into these states in the absence of noise because of their different symmetries. Since the fluctuations of A_1 and A_2 violate the symmetry with respect to exchange of donors 1 and 2, they make this excitation possible. The different shapes of the curves representing $|C_1(t)|^2$ and $|C_2(t)|^2$ are explained by the 'restructuring' of the eigenstate $|E_4\rangle$ at $J = \mu_B B/2$: the noise-induced transitions are accompanied by flipping one nuclear spin and one electron spin in opposite directions. Noise also contributes to a probability of transition to $|E_3\rangle$.

Figure 5 shows the dependence of the final amplitude of the $|E_4\rangle$ state on the duration of the measurement (solid curve). For small times T, the probability $P_4 = |C_4|^2 \to 0$ because the short-term dynamics of the electrons is only weakly affected by the hyperfine interaction, and the electron subsystem retains its spin during the course of the measurement. For sufficiently large times T, P_4 tends to 1 according to the law

$$1 - |C_4|^2 \propto \exp(-T/\tau).$$

For the representative values $B = 2$ T and $A/h = 2.9 \times 10^7$ Hz, one obtains $\tau^{-1} = 5.7 \times 10^5$ s^{-1}.

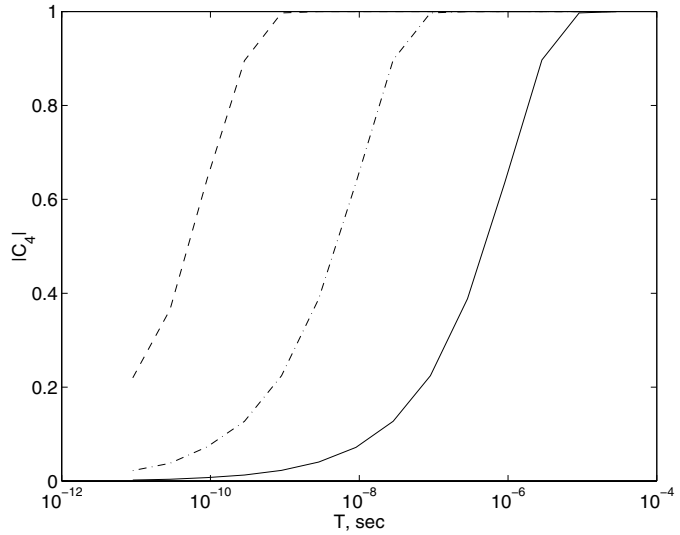

Figure 5. The amplitude of $|E_4\rangle$ versus the duration of the measurement for $B = 2$ T and $A/h = 2.9\times10^7$ Hz (solid curve). The dash–dotted and dashed curves show the same dependences for $A/h = 2.9 \times 10^8$ Hz and $A/h = 2.9 \times 10^9$ Hz, respectively.

To understand why τ^{-1} is three orders of magnitude smaller than A, we calculated the same curve for $A/h = 2.9 \times 10^8$ Hz and $A/h = 2.9 \times 10^9$ Hz (dash–dotted and dashed curves). Figure 6 shows the logarithmic plot of τ^{-1} versus A. By scaling A, we found that $\tau^{-1} \propto A^2/2\mu_B B\hbar$. This result can be readily explained. The width of the gap between the states $|E_4\rangle$ and $|E_3\rangle$ is $\Delta E = 4A$ (see figure 2, inset), and the corresponding interval of J is also of the order of A. Hence $T/\tau \sim \Delta E\, \Delta t/\hbar$, where Δt is the time of passage of the system through the bottleneck region.

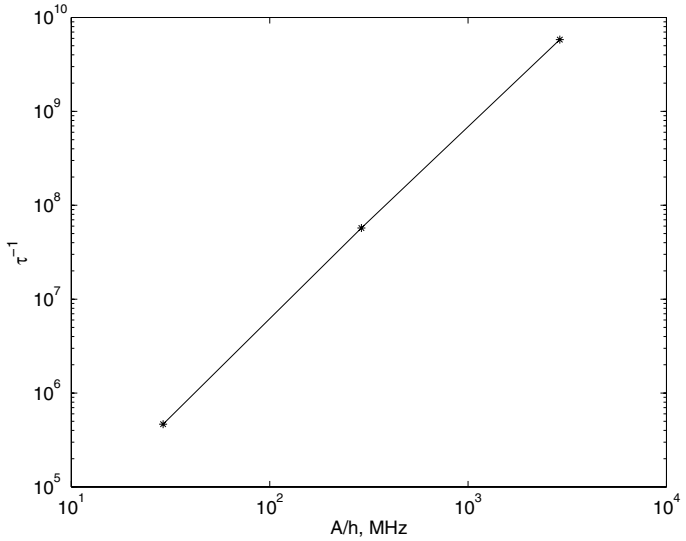

Figure 6. The characteristic time τ versus the hyperfine interaction constant A.

If it were not for the gate-voltage noise, the measurement error could be made vanishingly small just by increasing the duration of the measurement. However, because of noise, the error passes through a minimum as a function of the duration and then increases again. The details of the behaviour of the measurement error are shown in figure 7. The minimum error $(1 - |C_4|^2)_{min}$ is proportional to the noise spectral density S_A (see figure 8) and is of the order of 10^{-6} for typical values of noise.

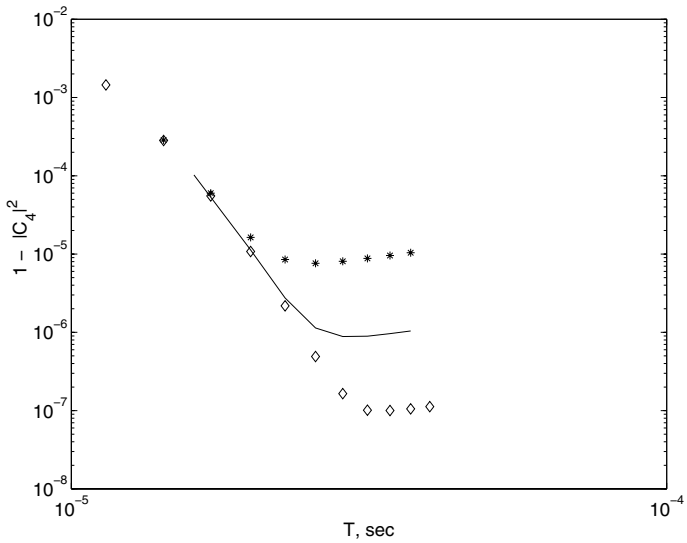

Figure 7. The measurement error, $1 - |C_4|^2$, versus the duration of the measurement for different levels of gate-voltage noise: $S_A/h^2 = 3.5 \times 10^{-3}$ Hz ($*$), 3.5×10^{-4} Hz (solid line), and 3.5×10^{-5} Hz ($\diamond$).

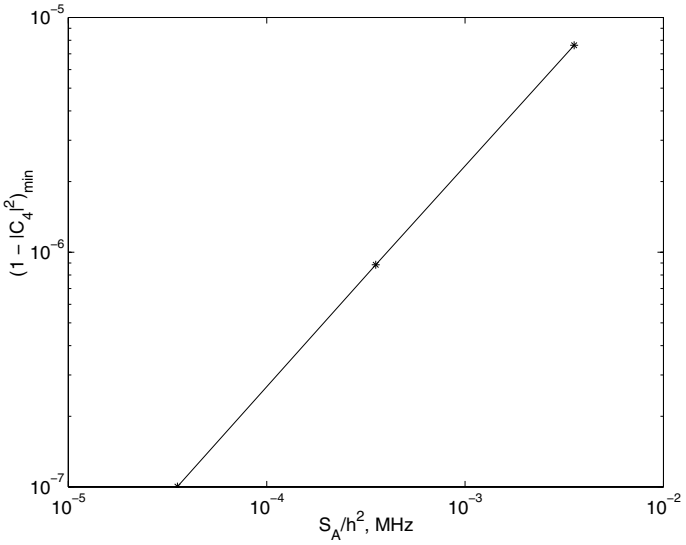

Figure 8. The minimum attainable measurement error versus the noise spectral density.

Acknowledgments

It is a pleasure to thank C Hammel, B Kane, and D Pelekhov for valuable discussions. KEN is grateful to the Theoretical Division and the CNLS of the Los Alamos National Laboratory for their hospitality. This work was supported by the National Security Agency, by the Department of Energy under contract W-7405-ENG-36, and by the Linkage Grant 93-1602 from the NATO Special Programme Panel on Nanotechnology.

References

[1] Kane B E 1998 *Nature* **393** 133
[2] Waugh J S and Slichter C P 1988 *Phys. Rev.* B **37** 4337
[3] Slichter C P 1996 *Principles of Magnetic Resonance* (Berlin: Springer)
[4] Enderlein R and Horing N J M 1997 *Fundamentals of Semiconductor Physics and Devices* (Singapore: World Scientific)
[5] Kohn W 1957 *Solid State Physics* vol 5, ed F Seitz and D Turnbull (New York: Academic)
[6] Kane B E, McAlpine N S, Dzurak A S, Clark R G, Milburn G J, Sun H B and Wiseman H 2000 *Phys. Rev.* B **61** 2961
[7] Abragam A 1961 *The Principles of Nuclear Magnetism* (Oxford: Oxford University Press)